Publ. Astron. Soc. Japan (2017) 69 (2), 37 (1–8)
doi: 10.1093/pasj/psx010
Advance Access Publication Date: 2017 March 10

Multi-color photometric investigation of the totally eclipsing binary NO Camelopardalis

Xiao Zhou,[1,2,3,*] Shengbang Qian,[1,2,3,4] and Bin Zhang[1,2,3,4]

[1]Yunnan Observatories, Chinese Academy of Sciences, 396 Yangfangwang, Guandu District, Kunming, 650216, P.R. China
[2]Key Laboratory for the Structure and Evolution of Celestial Objects, Chinese Academy of Sciences, 396 Yangfangwang, Guandu District, Kunming, 650216, P.R. China
[3]Center for Astronomical Mega-Science, Chinese Academy of Sciences, 20A Datun Road, Chaoyang District, Beijing, 100012, P.R. China
[4]Graduate University of the Chinese Academy of Sciences, Yuquan Road 19, Sijingshang Block, 100049 Beijing, P.R. China

*E-mail: zhouxiaophy@ynao.ac.cn

Received 2017 December 2; Accepted 2017 January 24

Abstract

Multi-color photometric light curves of NO Camelopardalis in V, R_C, and I_C bands are obtained and analyzed simultaneously using the Wilson–Devinney program. The solutions suggest that NO Cam is an A-subtype overcontact binary with a mass ratio of $q = 0.439$ and a contact degree of $f = 55.5\%$. The small temperature difference ($\Delta T = 44$ K) between its two components indicates that the system is under thermal contact. The high orbital inclination ($i = 84\overset{\circ}{.}5$) strengthens our confidence in the parameters determined from the light curves. All available times of minimum light are collected and period variations are analyzed for the first time. The $O - C$ curve reveals that its period is increasing continuously at a rate of $dP/dt = +1.46 \times 10^{-9}$, which can be explained by mass transfer from the less massive component to the more massive one. After the upward parabolic variation is subtracted, the residuals suggest that there may be a cyclic variation with a period of 2.23 yr and an amplitude of $A_3 = 0.00153$ d, which may due to the light-travel-time effect arising from the gravitational influence of a close-in tertiary component. The close-in companion reveals that early dynamic interaction among a triple system may have played a very important role in the formation of the W UMa-type binaries.

Key words: binaries: close — binaries: eclipsing — stars: individual (NO Camelopardalis)

1 Introduction

The formation and evolutionary theory of W UMa-type binaries is still an open issue. The most widely held view is that they are formed from initially detached binaries through nuclear evolution and angular momentum loss in the pre-contact phase. They will ultimately coalesce into single rapidly rotating stars, which may be progenitors of the poorly understood blue stragglers, FK Com-type stars, fast rotating A or F dwarf stars, and so on (Bradstreet & Guinan 1994). It has been demonstrated that the eruption of V1309 Sco was the result of a cool overcontact binary's merger (Nandez et al. 2014). Binnendijk (1970) divided the W UMa-type binaries into A and W subtypes. For A-subtype systems, the more massive component is the

Table 1. Coordinates of NO Cam, UCAC4 827-007726, and UCAC4 827-007718.

Targets	Name	$\alpha_{J2000.0}$	$\delta_{J2000.0}$	V_{mag}
Variable	NO Cam	$04^h14^m51\overset{s}{.}4$	$+75°20'40\overset{''}{.}7$	12.28
Comparison	UCAC4 827-007726	$04^h15^m56\overset{s}{.}4$	$+75°21'40\overset{''}{.}1$	12.55
Check	UCAC4 827-007718	$04^h15^m45\overset{s}{.}1$	$+75°17'14\overset{''}{.}6$	12.38

hotter one, while the less massive component is the hotter one in W-subtype systems.

Furthermore, more and more binaries are found in triple or multiple systems (Liao & Qian 2010) and several binaries with close-in companions have been reported recently (Qian et al. 2015), which makes the formation and evolutionary process of W UMa-type binaries more complex. Therefore, detailed light curve and orbital period analysis of W UMa-type binaries are still needed, which will provide invaluable information for the formation and evolutionary scenario of overcontact binaries.

NO Cam (= NSV 1495, $V = 12\overset{m}{.}28$) is a newly discovered variable star observed by the ROTSE All-Sky Survey I (Akerlof et al. 2000). It was listed as NSV 1495 in the NSV Catalogue (Blattler & Diethelm 2006), pointing out that it was a W UMa-type overcontact binary with spectral type F5. Since then, several times of minimum light have been published (e.g., Blattler & Diethelm 2006; Diethelm 2009; Nelson 2010). However, there is currently no spectroscopic element, photometric solution, or period research. In the present paper, V-, R_C-, and I_C-band light curves are analyzed using the Wilson–Devinney program and reliable photometric parameters are obtained. All times of minimum light are collected and the period variations are determined. The dynamic interaction and evolutionary scenario are discussed to understand the nature of W UMa-type binaries.

2 Multi-color CCD photometric observations

Multi-color light curve observations were carried out on 2013 January 13 and March 15 using the 85 cm reflecting telescope at Xinglong Observation Base, National Astronomical Observatories, Chinese Academy of Sciences. The telescope is located about 960 m above sea level. An Andor DW436 1K CCD camera is attached to the telescope. The effective field of view is $16\overset{'}{.}5$ by $16\overset{'}{.}5$, corresponding to a plate scale of 0.97 arcsec pixel^{-1} (Zhou et al. 2009). The operating temperature of the CCD camera was set to be -55°C. The broadband Johnson–Cousins V, R_C, I_C filters were used during the observations. UCAC4 827-007726 and UCAC4 827-007718 were chosen as the comparison star (C) and the check star (Ch), respectively. Their coordinates and V-band magnitudes are listed in table 1; the finding chart is shown in figure 1. The same integration time for the observations on January 13 and March 15 was used: 30 s for V band, 20 s for R_C band, and 15 s for I_C band. Since the comparison and check stars are very close to the target, the extinction differences were negligible. The PHOT package in IRAF[1] was used to process the observational images. The average observational errors were 0.003 mag (V), 0.002 mag (R_C), and 0.002 mag (I_C). A differential aperture photometry method is applied to determine the light variations. The light curves are displayed in figure 2 and a few lines of the observational data are shown in table 2. The standard deviations of the C and Ch data are all 0.008 mag for the V, R_C, I_C bands. The observational HJD are converted to phase with the following linear ephemeris:

$$\text{Min.I(HJD)} = 2456306.2287 + 0\overset{d}{.}430754 \times E. \quad (1)$$

Six CCD times of minimum light were determined, and the averaged values are listed in table 3.

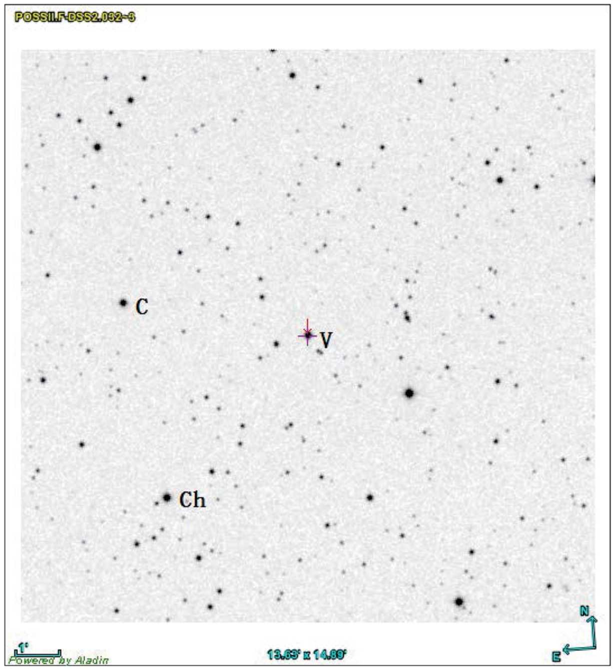

Fig. 1. Finding chart. (Color online)

[1] The Image Reduction and Analysis Facility is hosted by the National Optical Astronomy Observatories in Tucson, Arizona at ⟨http://iraf.noao.edu⟩.

Table 2. Observational data.*

HJD 2456300+	Phase	Δm	HJD 2456300+	Phase	Δm	HJD 2456300+	Phase	Δm
5.9466	0.3451	−0.056	5.9563	0.3676	− 0.009	5.9659	0.3899	0.050
5.9476	0.3474	−0.052	5.9573	0.3699	0.003	5.9668	0.3920	0.059
5.9485	0.3495	−0.049	5.9582	0.3720	0.006	5.9678	0.3943	0.065
5.9495	0.3518	−0.042	5.9592	0.3744	0.007	5.9688	0.3966	0.073
5.9505	0.3542	−0.037	5.9601	0.3764	0.016	5.9697	0.3987	0.073
5.9515	0.3565	−0.034	5.9611	0.3788	0.023	5.9707	0.4011	0.086
5.9525	0.3588	−0.019	5.9621	0.3811	0.026	5.9716	0.4031	0.097
5.9534	0.3609	−0.005	5.9630	0.3832	0.036	5.9726	0.4055	0.094
5.9544	0.3632	−0.009	5.9640	0.3855	0.035	5.9735	0.4076	0.110
5.9554	0.3655	−0.013	5.9649	0.3876	0.047	5.9760	0.4134	0.127

*These are only a few lines of the observational data; the entire dataset is available as "Supporting Information" in the online version of this paper.

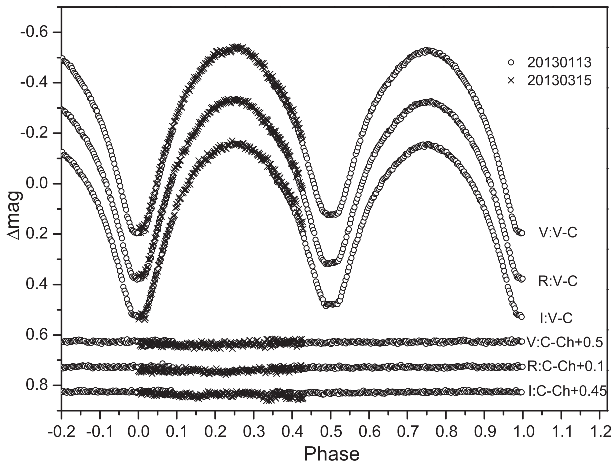

Fig. 2. Observed light curves. Open circles and crosses refer to data observed on January 13 and March 15, respectively.

3 Orbital period investigation

The $O - C$ method is the traditional way to reveal variations of orbital period. In the present work, a total of 16 CCD times of minimum light are collected, as listed in table 4, where "p" refers to the primary minimum and "s" refers to the secondary minimum. The initial residuals (Residuals$_1$) from equation (2) are listed in the fourth column of table 4:

$$\mathrm{Min.I(HJD)} = 2455480.8973 + 0\overset{\mathrm{d}}{.}430754 \times E. \tag{2}$$

When a quadratic curve is applied to the initial residuals, Residuals$_2$ are obtained and a periodic variation appears, as displayed in the middle of figure 3. Therefore, a sinusoidal term is superimposed on the ephemeris. Based on the least-squares method with the data weighted equally,

Table 3. New CCD times of minimum light.

JD (Hel.)	Error (d)	Min.	Filter	Telescope*
2456228.2601	±0.0008	I	BVR_CI_C	60 cm
2456301.2753	±0.0003	II	VR_CI_C	85 cm
2456306.0135	±0.0001	II	VR_CI_C	85 cm
2456306.2287	±0.0001	I	VR_CI_C	85 cm
2456351.0276	±0.0001	I	VR_CI_C	85 cm
2456630.1596	±0.0001	I	I_CN	1 m

*60 cm and 1 m denote the 60 cm and 1 m reflecting telescope at Yunnan Observatories; 85 cm denotes the 85 cm reflecting telescope at Xinglong Observation base.

the revised ephemeris is

$$\begin{aligned}\mathrm{Min.I} = {} & 2455480.8975(\pm 0.0001)\\ & + 0.43075666(\pm 0.00000006) \times E\\ & + 3.15(\pm 0.08) \times 10^{-10} \times E^2\\ & + 0.00153(\pm 0.00015)\sin[0.191(\pm 0.001)\\ & \times E - 20.9(\pm 4.2)].\end{aligned} \tag{3}$$

We conclude that the period is increasing continuously, at a rate of $dP/dt = +1.46 \times 10^{-9}$, and the periodic change span is $P_3 = 2.2$ yr with an amplitude of $A_3 = 0.00153$ d. The results from equation (3) are displayed in figure 3.

Since the first data ($E = -9247$) listed in table 4 is quite far away from the others, we remove it and do another trial. The most probable ephemeris is:

$$\begin{aligned}\mathrm{Min.I} = {} & 2455480.8974(\pm 0.0001)\\ & + 0.4307565(\pm 0.0000001) \times E\\ & + 4.33(\pm 0.58) \times 10^{-10} \times E^2\\ & + 0.00150(\pm 0.00014)\\ & \times \sin[0.189(\pm 0.001) \times E - 17.0(\pm 4.5)].\end{aligned} \tag{4}$$

Table 4. Times of minimum light.

JD(Hel.) (2400000+)	p/s	Epoch	Residuals	Error	Reference
51497.7180	p	− 9247	0.00294		Blattler and Diethelm (2006)
54833.6883	s	− 1502.5	− 0.00111	0.0004	Diethelm (2009)
55108.9387	s	− 863.5	− 0.00252	0.0001	Nelson (2010)
55127.8930	s	− 819.5	− 0.0014	0.0002	Diethelm (2010)
55480.8973	p	0	0	0.0002	Diethelm (2011)
55590.3107	p	254	0.00188	0.0020	Hubscher (2011)
55590.5256	s	254.5	0.00141	0.0016	Hubscher (2011)
55592.2489	s	258.5	0.00169	0.0010	Hubscher (2011)
55599.3562	p	275	0.00155	0.0008	Hubscher (2011)
55599.5705	s	275.5	0.00047	0.0014	Hubscher (2011)
55627.3569	p	340	0.00324	0.0047	Hubscher, Lehmann, and Walter (2012)
55627.5705	s	340.5	0.00146	0.0042	Hubscher, Lehmann, and Walter (2012)
55670.4308	p	440	0.00174	0.0037	Hubscher, Lehmann, and Walter (2012)
55863.8420	p	889	0.00439	0.0004	Hubscher, Lehmann, and Walter (2012)
56228.2601	p	1735	0.00461	0.0008	The present work
56230.8428	p	1741	0.00279	0.0019	Diethelm (2013)
56301.2753	s	1904.5	0.00701	0.0003	The present work
56306.0135	s	1915.5	0.00691	0.0001	The present work
56306.2287	p	1916	0.00674	0.0001	The present work
56342.4110	p	2000	0.0057	0.0008	Hoňková et al. (2013)
56351.0276	p	2020	0.00722	0.0001	The present work
56630.1596	p	2668	0.01063	0.0001	The present work

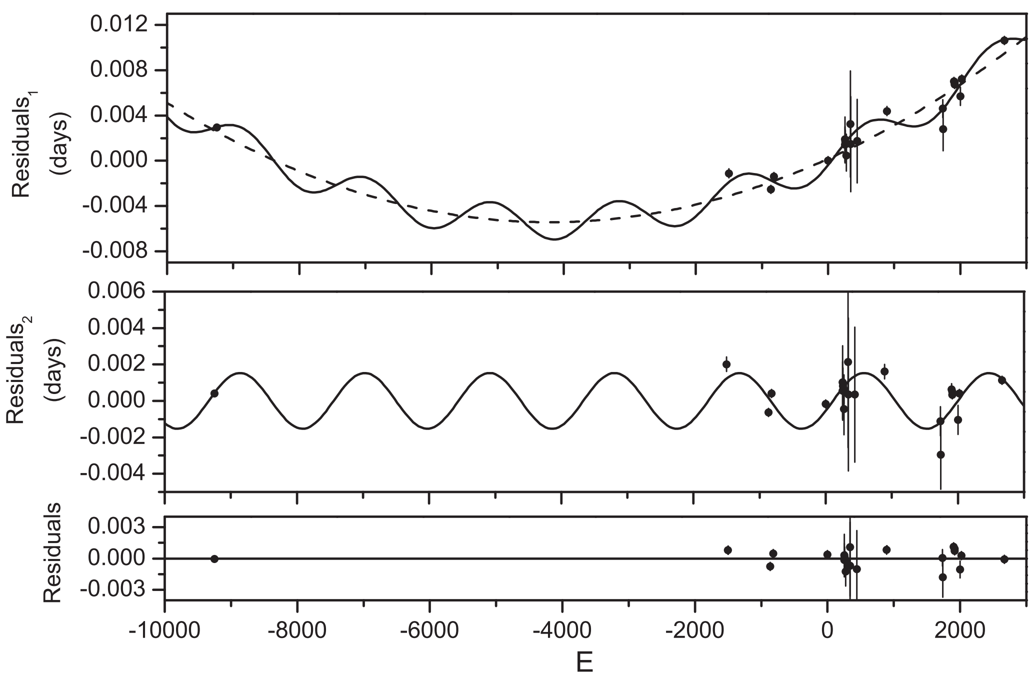

Fig. 3. In the upper panel, the dots represent the initial residuals calculated from equation (2). The solid line is the theoretical curve corresponding to equation (3), which contains an upward parabolic variation and a cyclic change, and the dashed line refers to the quadratic term in the equation. In the middle panel, the quadratic part from equation (3) is subtracted to make the periodic change clearer. The residuals are plotted in the bottom panel when both the upward parabolic change and the cyclic variation are removed.

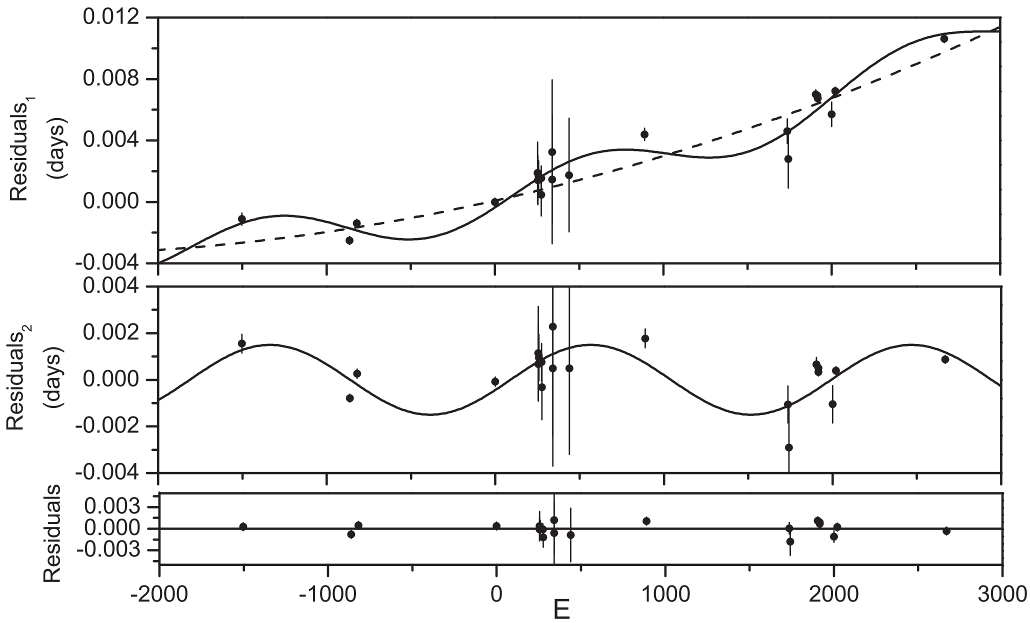

Fig. 4. $O - C$ curve from equation (4).

The results also determined a continuous period increase ($dP/dt = +2.01 \times 10^{-9}$) and a cyclic period change ($P_3 = 2.25$ yr, $A_3 = 0.00150$ d), as shown in figure 4.

Comparing the results from equation (3) with equation (4), we can conclude that the quadratic term makes little difference, but the periodic parts are almost the same. To check the reliability of the results, more times of minimum light are still needed in the future. We will adopt the results from equation (3) for further discussion in the paper hereafter.

4 Photometric solutions

As shown in figure 2, the light curves vary continuously, and the depth of the primary and secondary minima are almost equal, which indicates that NO Cam is a typical W UMa-type overcontact binary. To derive its physical parameters, the 2013 version of the Wilson–Devinney program (Wilson & Devinney 1971; Van Hamme & Wilson 2007; Wilson et al. 2010) is used. The number of observational data used in the program are 444 in the V band, 445 in the R_C band, and 437 in the I_C band. The observational HJD were converted to phase while applying the program.

The spectral type given in the NSV Catalogue (Blattler & Diethelm 2006) is F5. The 2MASS All Sky Catalogue (Cutri et al. 2003) gives a color index of $J - H = 0.220$, which also corresponds to a spectral type of F5. Thus, the effective surface temperature of the primary star (the star eclipsed at primary minimum) is set to be $T_1 = 6530$ K (Cox 2000). Convective atmospheres are assumed, and the corresponding gravity-darkening coefficients of $g_1 = g_2 = 0.32$ (Lucy 1967) and bolometric albedo of $A_1 = A_2 = 0.5$ (Ruciński 1969) are assigned. The limb-darkening coefficients originate from the table in Van Hamme (1993) by considering a logarithmic law accordingly.

Mode 3 for the contact system is adopted. As it is a total eclipsing binary, the mass ratio will be well-determined from light curves since the amplitude of light variation depends mainly on the mass ratio for total annular eclipsing binaries, whereas the amplitude also depends strongly on inclination (Terrell & Wilson 2005) for partial eclipses. The adjustable parameters are: mass ratio q (M_2/M_1); orbital inclination i; effective temperature of the secondary star T_2; monochromatic luminosity of the primary star L_{1V}, L_{1R}, and L_{1I}; the dimensionless potential of the primary and secondary stars ($\Omega_1 = \Omega_2$ in this case); and the third light l_3. In our solutions, we find that the contribution of third light is negligible. The converged photometric solutions are listed in table 5, Solutions A. The theoretical light curves are displayed in figure 5. The standard deviations of the fitting residuals are 0.009 mag (V), 0.007 mag (R_C), and 0.007 mag (I_C).

Since the light curves show very good symmetry and Solutions A for convective parameters imply that there may be no spot on the stars, radiative parameters of $g_1 = g_2 = 1.00$ (Lucy 1967) and $A_1 = A_2 = 1.00$ (Ruciński 1969) are tried, and Solutions B is obtained in table 5. The theoretical light curves for Solutions B is almost the same as those in figure 5, so they are not displayed here. Comparing Solutions A with Solutions B, it is found that the convective parameters determine a smaller temperature difference and residual, which may be much more

Table 5. Photometric solutions.

Parameters	Solutions A	Solutions B
$T_1(K)$	6530(fixed)	6530(fixed)
g_1	0.32(fixed)	1.00(fixed)
g_2	0.32(fixed)	1.00(fixed)
A_1	0.50(fixed)	1.00(fixed)
A_2	0.50(fixed)	1.00(fixed)
$a\,(R_\odot)$	3.03(fixed)	3.02(fixed)
q (M_2/M_1)	0.439(±0.001)	0.416(±0.001)
$i\,(^\circ)$	84.5(±0.1)	83.8(±0.1)
$\Omega_1 = \Omega_2$	2.6099(±0.0036)	2.6097(±0.0036)
T_2 (K)	6486(±3)	6304(±4)
ΔT (K)	44	226
T_2/T_1	0.9933(±0.0005)	0.9654(±0.0006)
$L_1/(L_1+L_2)$ (V)	0.6731(±0.0002)	0.7141(±0.0003)
$L_1/(L_1+L_2)$ (R_C)	0.6721(±0.0003)	0.7094(±0.0003)
$L_1/(L_1+L_2)$ (I_C)	0.6713(±0.0003)	0.7052(±0.0003)
r_1 (pole)	0.4527(±0.0005)	0.4483(±0.0005)
r_1 (side)	0.4896(±0.0006)	0.4830(±0.0006)
r_1 (back)	0.5298(±0.0008)	0.5179(±0.0007)
r_2 (pole)	0.3189(±0.0015)	0.3053(±0.0014)
r_2 (side)	0.3378(±0.0019)	0.3216(±0.0018)
r_2 (back)	0.3986(±0.0044)	0.3713(±0.0036)
f	55.5%(±1.4%)	39.6%(±1.4%)
$\Sigma\omega(O-C)^2$	0.005229	0.005288

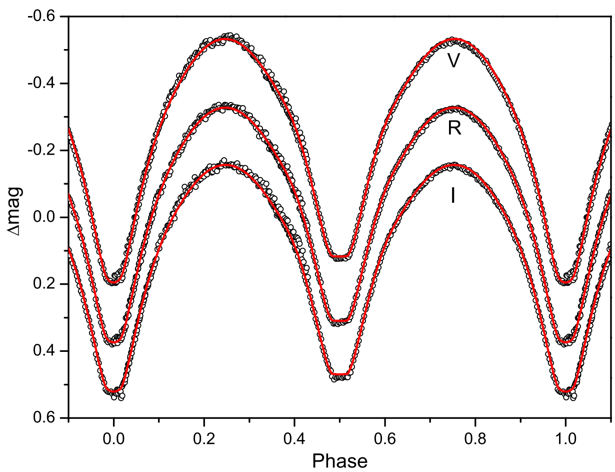

Fig. 5. Light curve comparison: Open circles refer to observed light curves and red lines correspond to theoretical light curves. (Color online)

acceptable. Solutions A will be used for further discussion hereafter.

5 Discussions and conclusions

The light curve solutions suggest that NO Cam is an A-subtype overcontact binary with a mass ratio of $q = 0.439$. The contact degree of $f = 55.5\%$ reveals that it is a deep contact system (Qian et al. 2005). The two components have nearly the same surface temperature ($\Delta T = 44$ K) in spite of their quite different masses and radii, which indicates that the system is under thermal contact. The primary component contributes about 67% of the total luminosity, and the existence of the third light (l_3) is not detected. The orbital inclination is $i = 84^\circ\!.5$, which confirms our assumption that NO Cam is a totally eclipsing binary, indicating that the photometric parameters are derived reliably. As there are no radial velocity curves, we cannot give a direct determination of the absolute parameters. Assuming that the primary component is a normal main-sequence star, its mass is estimated to be $M_1 = 1.4\,M_\odot$ (Cox 2000). Considering the mass ratio obtained, the mass of the secondary star is calculated to be $M_2 = 0.61\,M_\odot$. The semi-major axis listed in table 5 is calculated according to the assumed masses. According to the statistical analysis conducted by Yang and Qian (2015), F-type contact binaries have a really high ratio in extreme mass ratio, overcontact binary systems. It is supposed that NO Cam may evolve into an extreme mass ratio, overcontact binary system and merge into a single rapidly rotating star as in the case of V1309 Sco (Nandez et al. 2014; Zhu et al. 2016).

The period analysis shows that its orbital period is increasing at a rate of $dP/dt = +1.46 \times 10^{-9}$. To account for the period increase, a conservative mass transfer mechanism is supposed. Applying the estimated masses to the well-known equation

$$\frac{dM_2}{dt} = -\frac{M_1 M_2}{3P(M_1 - M_2)} \times dP/dt, \tag{5}$$

we conclude that the period increase is due to mass transfer from the less massive component to the more massive one. The mass transfer rate is $\frac{dM_2}{dt} = 8.37 \times 10^{-8}\,M_\odot\,\mathrm{yr}^{-1}$. However, the real mass transfer rate may be quite different from this value when the contribution of angular momentum loss is considered.

As shown in the middle panel of figure 3, there may be a cyclic variation superimposed on the period variations. Cyclic oscillations are usually encountered for W UMa-type overcontact binary stars (Qian 2003), which could be plausibly explained as the light-travel-time effect arising from the gravitational influence of a third object (Liao & Qian 2010). By assuming a circular orbit, the projected orbital radius rotating around the barycenter of the triple system is calculated with the equation

$$a'_{12}\sin i' = A_3 \times c, \tag{6}$$

where A_3 is the amplitude of periodic variation and c is the speed of light. Therefore, the projected orbital radius is calculated to be $a'_{12}\sin i' = 0.26(\pm 0.02)$ au. Considering the mass function of the triple system and the masses of the

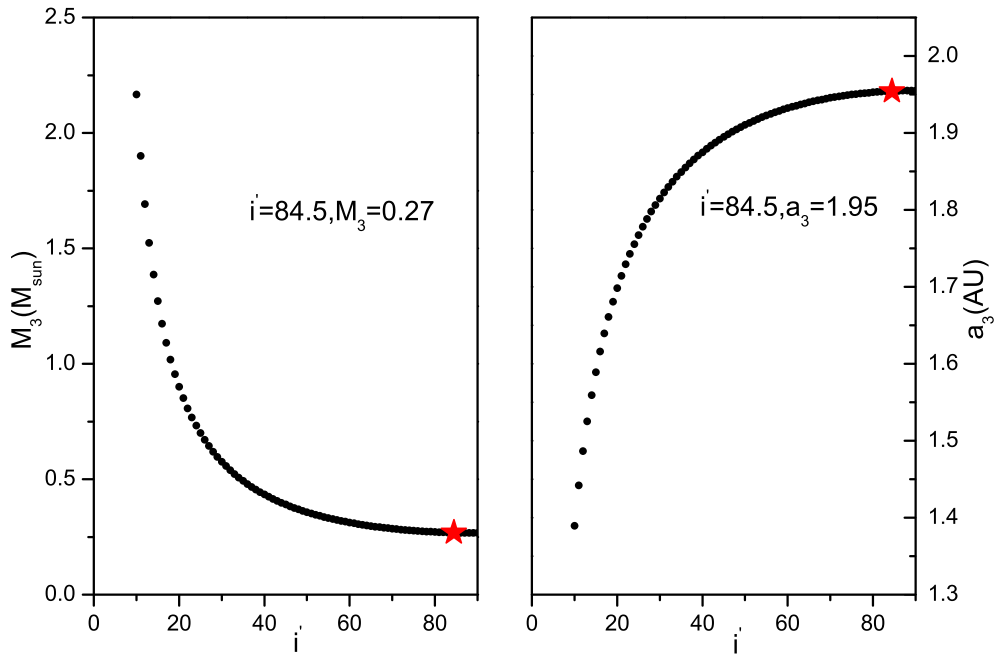

Fig. 6. Left panel: Relation between the mass M_3 (in units of $M_\odot$) of the third component and its orbital inclination i' (°). Right panel: Relations between the orbital radius a_3 (in units of au) of the third component and its orbital inclination i' (°). The red star is the position of the tertiary component when it is coplanar with NO Cam. (Color online)

primary and secondary stars, the mass and orbital radius of the tertiary companion are computed with the equation

$$f(m) = \frac{4\pi^2}{GP_3^2} \times (a'_{12} \sin i')^3 = \frac{(M_3 \sin i')^3}{(M_1 + M_2 + M_3)^2}, \qquad (7)$$

where G is the gravitational constant and P_3 is the period that the tertiary component orbits around NO Cam. The mass function is calculated to be $f(m) = 0.00373\ M_\odot$. The i'–M_3 and i'–a_3 diagrams are shown in figure 6, where the red stars are the mass and orbital radius of the tertiary component when the three components are coplanar.

Although tertiary components are quite common in W UMa systems, their effects on the hosting binaries are not clear. They supposedly accelerate the orbital evolution of the hosting binary by removing angular momentum from it during the early dynamical interaction (Qian et al. 2013, 2014b). According to our calculation, NO Cam is a triple system with a cool stellar companion at an orbital separation of about 1.95 au. Recently, some binaries with close-in companions have been reported, as listed in table 6. It should be mentioned that the masses are minimum values since we do not know the orbital inclination (i') of the tertiary components. The most special one is CSTAR 038663, in which the tertiary component is only about 1 au from the central binary system. Dynamic interaction among the triple system must have a significant influence on the formation of the binary system. Contact binaries with close-in companions are important targets for testing theories of star formation and interaction, and should be studied over the long term.

Table 6. Parameters of close-in companions to contact binaries ($i' = 90°$).

Target	M_3 ($M_\odot$)	a_3 (au)	Reference
PY Vir	0.79	2.8	Zhu et al. (2013a)
V401 Cyg	0.70	2.4	Zhu et al. (2013b)
CSTAR 038663	0.63	0.93	Qian et al. (2014a)
SDSS J001641−000925	0.14	2.8	Qian et al. (2015)
V384 Ser	0.37	2.0	Liao et al. (2015)
NO Cam	0.27	1.96	The present work

Acknowledgement

This work is supported by the Chinese Natural Science Foundation (Grant Nos. 11133007, 11325315, 11203066 and 11403095), the Strategic Priority Research Program "The Emergence of Cosmological Structure" of the Chinese Academy of Sciences (Grant No. XDB09010202), and the Science Foundation of Yunnan Province (Grant Nos. 2012HC011 and 2014FB187). New CCD photometric observations of NO Cam were obtained with the 60 cm and 1.0 m telescopes at Yunnan Observatories, and the 85 cm telescope at Xinglong Observation base in China. This research has made use of the SIMBAD database, operated at CDS, Strasbourg, France, and the fourth US Naval Observatory CCD Astrograph Catalog (UCAC4).

Supporting information

Supplementary data are available at *PASJ* online.

Complete dataset of table 2.

References

Akerlof, C., et al. 2000, AJ, 119, 1901
Binnendijk, L. 1970, VA, 12, 217
Blattler, E., & Diethelm, R. 2006, IBVS, 5699
Bradstreet, D. H., & Guinan, E. F. 1994, ASP Conf. Ser., 56, Interacting Binary Stars ed. A. W. Shafter (San Francisco: ASP), 228
Cox, A. N. ed. 2000, Allen's Astrophysical Quantities, 4th ed. (New York: Springer)
Cutri, R. M., et al. 2003, VizieR Online Data Catalog, II/246
Diethelm, R. 2009, IBVS, 5894
Diethelm, R. 2010, IBVS, 5920
Diethelm, R. 2011, IBVS, 5960
Diethelm, R. 2013, IBVS, 6042
Hoňková, K., et al. 2013, Open Eur. J. Variable Stars, 0160
Hubscher, J. 2011, IBVS, 5984
Hubscher, J., Lehmann, P. B., & Walter, F. 2012, IBVS, 6010
Liao, F. M. W., Qian, S., Zhu, L., & Liu, L. 2015, Pub. Korean Astron. Soc., 30, 215
Liao, W.-P., & Qian, S.-B. 2010, MNRAS, 405, 1930
Lucy, L. B. 1967, ZAp, 65, 89
Nandez, J. L. A., Ivanova, N., & Lombardi, J. C., Jr. 2014, ApJ, 786, 39
Nelson, R. H. 2010, IBVS, 5929
Qian, S. 2003, A&A, 400, 649
Qian, S.-B., et al. 2013, ApJS, 209, 13
Qian, S.-B., et al. 2014a, ApJS, 212, 4
Qian, S.-B., et al. 2015, ApJ, 798, L42
Qian, S.-B., Yang, Y.-G., Soonthornthum, B., Zhu, L.-Y., He, J.-J., & Yuan, J.-Z. 2005, AJ, 130, 224
Qian, S.-B., Zhou, X., Zola, S., Zhu, L.-Y., Zhao, E.-G., Liao, W.-P., & Leung, K.-C. 2014b, AJ, 148, 79
Ruciński, S. M. 1969, Acta Astron., 19, 245
Terrell, D., & Wilson, R. E. 2005, Ap&SS, 296, 221
Van Hamme, W. 1993, AJ, 106, 2096
Van Hamme, W., & Wilson, R. E. 2007, ApJ, 661, 1129
Wilson, R. E., & Devinney E. J., 1971, ApJ, 166, 605
Wilson, R. E., Van Hamme, W., & Terrell, D. 2010, ApJ, 723, 1469
Yang, Y.-G., & Qian, S.-B. 2015, AJ, 150, 69
Zhou, A.-Y., Jiang, X.-J., Zhang, Y.-P., & Wei, J.-Y. 2009, Res. Astron. Astrophys., 9, 349
Zhu, L. Y., Qian, S. B., Liu, N. P., Liu, L., & Jiang, L. Q. 2013a, AJ, 145, 39
Zhu, L.-Y., Qian, S.-B., Zhou, X., Li, L.-J., Zhao, E.-G., Liu, L., & Liu, N.-P. 2013b, AJ, 146, 28
Zhu, L.-Y., Zhao, E.-G., & Zhou, X. 2016, Res. Astron. Astrophys., 16, 016